Liquid Crystals
Publication details, including instructions for authors and subscription information:
http://www.informaworld.com/smpp/title~content=t713926090

Slow relaxation processes in nematic liquid crystals at weak surface anchoring

S. V. Pasechnik[a]; V. G. Chigrinov[b]; D. V. Shmeliova[a]; V. A. Tsvetkov[a]; V. N. Kremenetsky[b]; Liu Zhijian[b]; A. V. Dubtsov[a]
[a] Moscow State Academy of Instrument Engineering & Computer Science, Stromynka 20, 107846 Moscow, Russia [b] Hong Kong University of Science & Technology, Clear Water Bay, Kowloon, Hong Kong

To cite this Article Pasechnik, S. V. , Chigrinov, V. G. , Shmeliova, D. V. , Tsvetkov, V. A. , Kremenetsky, V. N. , Zhijian, Liu and Dubtsov, A. V.(2006) 'Slow relaxation processes in nematic liquid crystals at weak surface anchoring', Liquid Crystals, 33: 2, 175 — 185
To link to this Article: DOI: 10.1080/02678290500277862
URL: http://dx.doi.org/10.1080/02678290500277862

Liquid Crystals, Vol. 33, No. 2, February 2006, 175–185

Taylor & Francis
Taylor & Francis Group

Slow relaxation processes in nematic liquid crystals at weak surface anchoring

S.V. PASECHNIK†, V.G. CHIGRINOV*‡, D.V. SHMELIOVA†, V.A. TSVETKOV†, V.N. KREMENETSKY‡, LIU ZHIJIAN‡ and A.V. DUBTSOV†

†Moscow State Academy of Instrument Engineering & Computer Science, Stromynka 20, 107846 Moscow, Russia
‡Hong Kong University of Science & Technology, Clear Water Bay, Kowloon, Hong Kong

(*Received 27 January 2005; in final form 1 May 2005; accepted 14 May 2005*)

We present new results of experimental investigations of azimuthal director reorientation dynamics for a nematic liquid crystal on solid substrates. Two types of substrate with weak anchoring were studied: glass/polystyrene and glass/UV-activated dye. Slow and fast relaxation processes were observed in both cases under the action of a strong 'in-plane' electric field. The slow surface reorientation and memory effects were controlled by two parameters: the electric voltage and the excitation time. It was established that the increase of the excitation time results in a slowing of the relaxation of the system to the initial state after turning off the electric field. A phenomenological model of a gliding of easy axes is proposed to explain the slow relaxation process.

1. Introduction

The nature of the surface anchoring of liquid crystals (LCs) in contact with solids and polymer films is of great interest as it plays a key role in display applications. Usually the preferred orientation of the long axis of the LC molecules on the solid-like surface in the absence of external fields is described in terms of an easy axis $\mathbf{n}_e$. The position of $\mathbf{n}_e$ corresponds to the minimum value of the surface anchoring energy and determines the behaviour of a liquid crystal director both in the vicinity of the surface (surface director $\mathbf{n}_s$) and in the bulk (bulk director $\mathbf{n}_b$) of a liquid crystal layer. Magnetic and electric fields can stimulate an extremely slow process, the so-called gliding of the LC director, which can be referred to as a slow rotation of the easy axes under external torques [1–3]. This process was observed for the azimuthal reorientation of easy axes for both lyotropic [2] and thermotropic [1] liquid crystals. Recent experiments with extremely thin (1.5 μm) layers of nematic liquid crystals distorted by strong electric fields ($\sim 3\,\mathrm{V}\,\mu\mathrm{m}^{-1}$) have shown that zenithal gliding is also possible in cells with strongly anchoring surfaces [4]. The gliding of the director shows very pronounced features of memory effect: the easy axis slowly relaxes to its initial position after removing the external torques. It is not yet clear if this phenomenon can be considered as completely reversible. The characteristic times vary from minutes up to days depending on the experimental conditions, so quasi-stationary memory effects remain for a long periods. The phenomena under consideration can play an essential role in LC application, as they may modify some technical displays parameters; for example, optical contrast, threshold voltage, etc. Thus both experimental and theoretical investigations of the gliding phenomena are very important.

Although experimental evidence of a gliding and field-induced memory in nematics has been obtained by various authors [1–5], these phenomena are not clearly understood. A number of alternative physical mechanisms (the field-induced reorientation of defect-like surface layer [2], the polymeric chains reorientation [5], a surface director motion [1], the absorption and desorption of mesogenic molecules [3]) have been proposed to explain the experimental results. Nevertheless, the phenomenological models developed provide only a qualitative description of the phenomena described, and additional experiments with different types of LC cells are needed for an appropriate explanation.

2. Experimental

In this paper we present new results on slow surface dynamics for two types of surface treatment that provide weak planar anchoring. In the first surface treatment a planar (or twist) orientation was achieved

*Corresponding author. Email: eechigr@ust.hk

Liquid Crystals
ISSN 0267-8292 print/ISSN 1366-5855 online © 2006 Taylor & Francis
http://www.tandf.co.uk/journals
DOI: 10.1080/02678290500277862

by rubbing a polystyrene film (PS treatment); the easy axis was oriented perpendicular to the rubbing direction. The UV photoalignment (PA) technique [6] was used in the second case. The main ideas of the experiment were similar to those described earlier [1]: namely, we used liquid crystal cells with (i) a strong planar surface anchoring and (ii) a weak anchoring, on opposing glass plates contacted via a LC layer. The direction of filling was the same as the direction of the LC easy axis. The initial orientation of LC after filling was controlled in the anisotropic phase at room temperature, as flow can create alignment defects, especially for very weak anchoring [6]. The general scheme of the LC cells is shown in figure 1.

We studied cells both with a variable thickness of nematic layer (20–50 μ) similar to that described previously for shear viscosity measurements [7], and with a fixed thickness. The first type provides a simultaneous study of field-induced orientation changes with variation of local thickness of a nematic layer. The LC cell with fixed layer thickness (d=18 μm) was treated by UV light so as to obtain zones with different energies of illumination, and thus with different anchoring strengths (figure 2).

A strong in-plane electric field (f=1…10 kHz) was formed in the narrow gaps (of width g=10 μm and 100 μm) between transparent indium tin oxide (ITO) electrodes placed on the glass plate with weak anchoring. These gaps were observed in polarized light as bright stripes, which showed memory effects after the electric field was turned off. A nematic mixture ZhK 616 (from NIOPIK, Moscow), with a positive value (+3.4) of dielectric permittivity anisotropy, was used for effective control via electric field application. The brightness of the stripe decreased very slowly under the appropriate choice of experimental conditions, showing some form of memory effect.

We used both (i) an image processing procedure to obtain the time dependence of brightness R of images inside the gap (R considered to be proportional to the

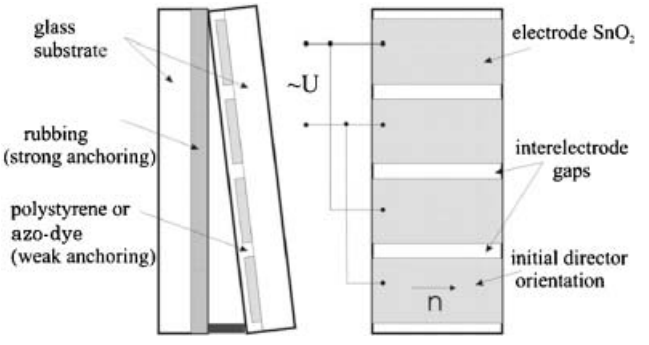

Figure 1. General scheme of LC cells.

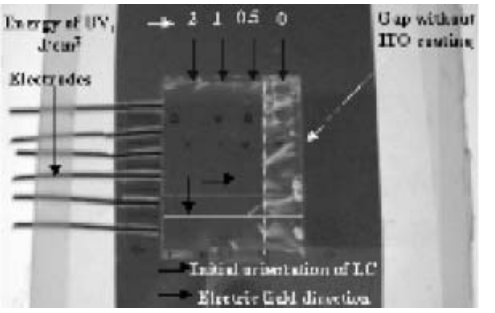

Figure 2. PA-treated cell of constant thickness; photomicrograph in crossed polarizers.

local intensity of light), and (ii) direct registration of the intensity $I(t)$ changes of a laser light, locally passing through the region of the gap. This provides a study of both fast and slow time variations of the optical properties of the LC layer. The measurement results depended on two control parameters: electric voltage U applied to the gap, and the excitation time t_{ex} (the time of electric field application).

3. Results and discussion

Examples of local images of the cell gaps with an initial planar orientation (PA technique), and with a twisted orientation (rubbed polystyrene) obtained after turning on the electric field and at different times after removing it are shown in figure 3. After the application of an a.c. electric field, the gaps between electrodes appeared in polarized light as narrow bright stripes, surrounded by a coloured region via some electric field scattering, figure 3 (a). Turning off the field results in a fast (few seconds) disappearance of the image except for the central part inside the gap. In this region both fast and very slow (some min to 20 h) variations of the brightness of the images were observed for the appropriate choice of experimental conditions (figures 3 and 4). The fast variations of the optical picture after turning off the field could be attributed to the usual bulk changes of LC orientation [6]. If the thickness of a nematic layer d=18 μm, corresponding to the images in figure 3 (a), the estimated characteristic time for the twist deformation $\tau_0=\gamma_1 d^2/K_{22}$ is about 5 s, which is in accordance with our observations, (γ_1 and K_{22} are LC rotation viscosity and twist elastic constant, d is the LC layer thickness).

The registered optical changes inside the gap depended essentially both on the voltage U, and on the time of its application, the excitation time t_{ex}. In particular, for PA treatment the optical picture in the gap with width g also relaxed to the initial dark state for some seconds after turning off the field, i.e. for $U/g<20$ V over 10 μm, $t_{ex}<10$ min, at the exposure

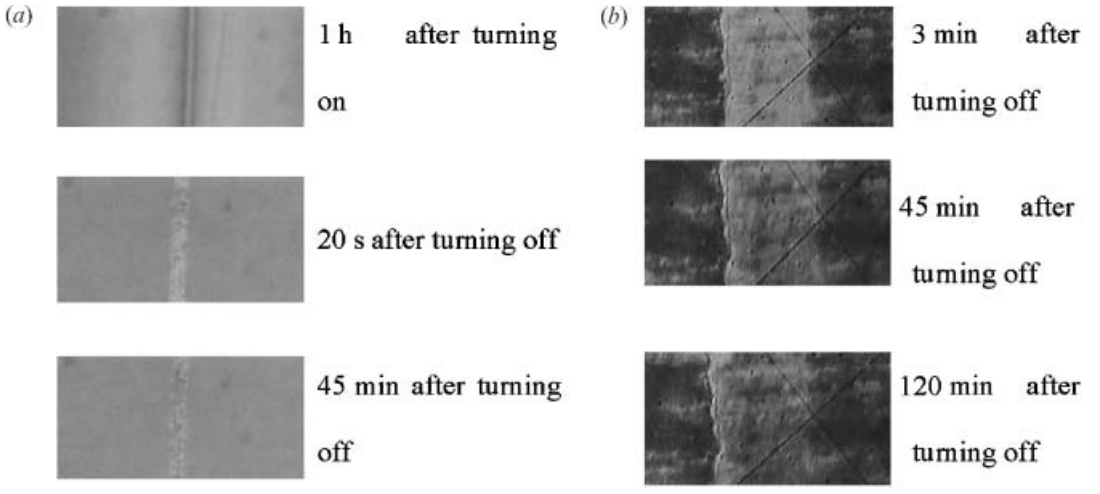

Figure 3. Microscopic images of the gaps for different moments of time. (*a*) Initial planar orientation (PA treatment), exposure energy $J=0.5\,\mathrm{J\,cm^{-2}}$, a.c. voltage ($f=10\,\mathrm{kHz}$) per width of the gap $U/g=30\,\mathrm{V}/10\,\mu\mathrm{m}$, excitation time $t_{ex}=1\,\mathrm{h}$. (*b*) Initial twisted orientation (PS treatment): $U/g=300\,\mathrm{V}/100\,\mu\mathrm{m}$, $f=5\,\mathrm{kHz}$, $t_{ex}=85\,\mathrm{min}$.

energy $J=0.5\,\mathrm{J\,cm^{-2}}$. Similar fast relaxation at sufficiently small values of U and t_{ex} were registered for the cell with a rubbed polystyrene surface, see figure 5.

Slow variations of image brightness and memory-like effects took place at higher values of U and t_{ex}. The character of such slow processes crucially depended on the excitation time t_{ex} at a fixed amplitude E ($E\cong U\,\mathrm{g^{-1}}$) of the applied electric field, see figure 6. The threshold excitation time required for slow relaxation increased with decreasing voltage and was about 5 h at $U=100\,\mathrm{V}$, $g=100\,\mu\mathrm{m}$ in the case of the polystyrene surface. Slow (more than 10 min) field-induced variation of the surface optical images of the cells treated both by the PA technique ($J\geqslant 0.5\,\mathrm{J\,cm^{-2}}$) and rubbing were observed for $2\,\mathrm{V\,\mu m^{-1}}\leqslant U\,\mathrm{g^{-1}}\leqslant 3\,\mathrm{V\,\mu m^{-1}}$ at $t_{ex}>1\,\mathrm{h}$ (figure 3). They appeared to be reversible, at least for excitation times below 2 h for the two types of surface treatment described.

Pronounced permanent memory effects were seen when t_{ex} exceeded 2 h (figures 7 and 8). In the case of a polystyrene surface, the memory effects could be considerably reduced by heating the LC to the isotropic phase and cooling it in the presence of a magnetic field (0.3 T) oriented along the initial direction of the easy axis (figure 9). The threshold values of E and t_{ex} for the appearance of memory effects depended drastically on the quality of the initial orientation. Usually inhomogeneity of the surface orientation results in a decrease of the threshold voltage.

Furthermore, we observed memory effects induced by low electric voltage even in the region of the cell untreated by UV radiation, where slight inhomogeneous

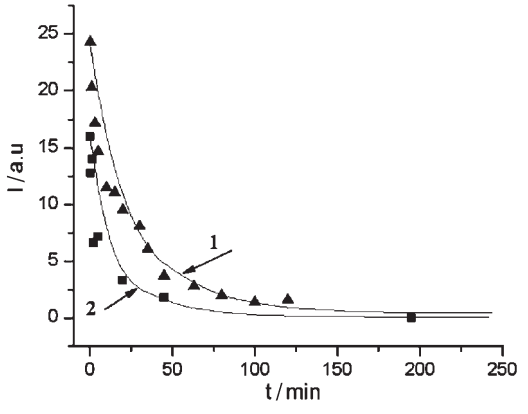

Figure 4. Time dependence of light intensity $I(t)$ obtained by processing the series of images presented in figure 3 with approximation lines by exponential law: $I(t)=A_0+A_1\exp(-t/\tau_1)+A_2\exp(-t/\tau_2)$. Curve 1: initial PS twist orientation, $\tau_1=1.57\,\mathrm{min}$, $\tau_2=35\,\mathrm{min}$; curve 2: initial PA planar orientation, $\tau_1=1.3\,\mathrm{min}$, $\tau_2=42\,\mathrm{min}$.

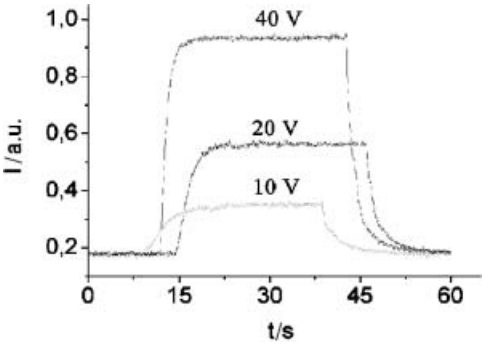

Figure 5. Time dependence of light intensity: turning on and turning off the electric field (fast relaxation process); initial planar orientation with PS treatment.

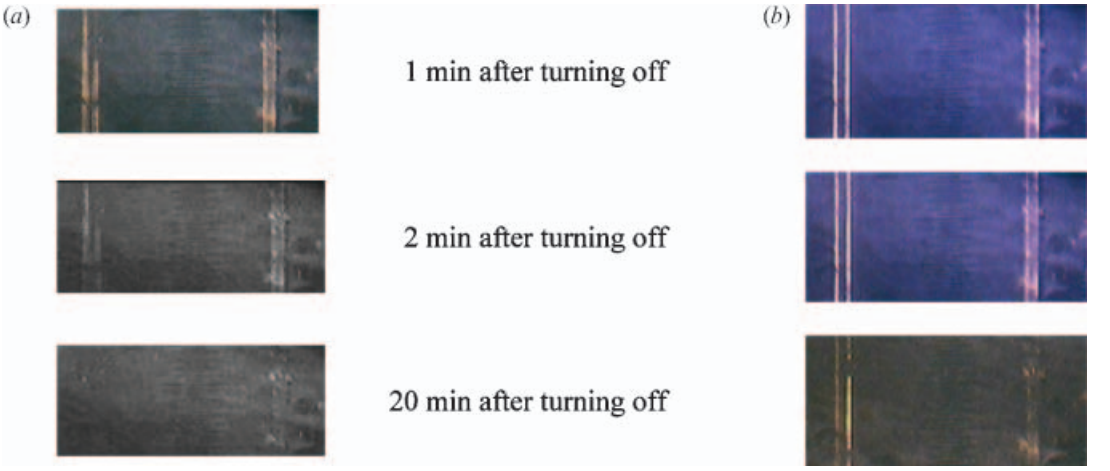

Figure 6. Images of a cell after turning off electric field; PA treatment, wedge-like cell, $d \cong 30\,\mu m$, $g = 100\,\mu m$, $J = 0.2\,J\,cm^{-2}$: (*a*) excitation time $t_{ex} = 35$ min; (*b*) $t_{ex} = 65$ min.

orientation was induced by flow during filling the cell with LC (figure 2). Similar results were reported for other types of weakly anchoring surface [3]. We suggest therefore that the slow relaxation processes and memory effects occur due to the interaction of a weakly anchoring layer of a dye (polymer) with both the solid substrate and the liquid crystal. We found no pronounced variation of the images with variation of the layer thickness in the range 20–50 µm. This confirms the surface-like nature of the slow relaxation processes observed.

In the case of PA treatment, the most pronounced memory effects were observed near the edges of the gaps due to the high field strength in the vicinity of these edges (figure 6). The images inside the gap also became inhomogeneous, figure 3 (*a*), at sufficiently high values of $t_{ex} \approx 1$ h and $V \geqslant 2\,V\,\mu m^{-1}$, $J = 0.5\,J\,cm^{-2}$. In the case of polystyrene rubbing, the images appeared more homogeneous, particularly for the initial twist orientation, figure 3 (*b*). We also found that the slow LC relaxation after turning off the field, and memory effects, depended on the exposure energy of UV irradiation and so presumably on the anchoring strength. Despite the inhomogeneous character of such phenomena we observed that in general they were suppressed on increasing the exposure energy.

4. Theoretical model

The simplest way to explain our results, including those on slow surface dynamics, is to apply the model of a LC layer as a number of sub-layers with different physical properties. A similar approach was previously proposed to describe the first results on 'in-plane' gliding of the LC director on a polymeric surface treated by UV radiation [1] and for polar gliding on substrates with rather strong anchoring [4]. Some assumptions of this model were recently discussed in the framework of a hydrodynamic theory [8].

We consider three different layers inside the LC cell, with different LC orientation determined by the

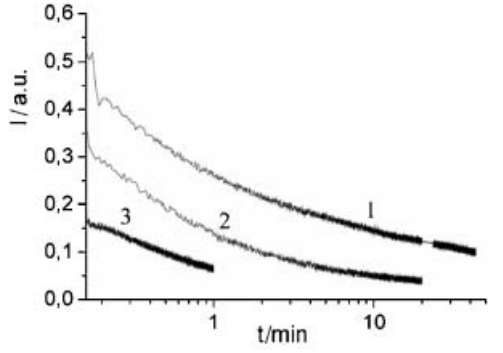

Figure 7. Time dependence of light intensity after turning off voltage: polystyrene, $U/g = 300\,V/100\,\mu m$, $f = 3$ kHz, $t_{ex}(1) = 133$ min, $t_{ex}(2) = 50$ min, $t_{ex}(3) = 25$ min.

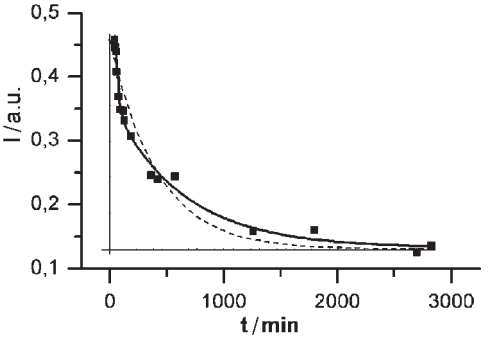

Figure 8. Transmission light intensity $I(t)$ after turning off voltage. PA treatment, $t_{ex} = 17$ h, $U/g = 300\,V/100\,\mu m$, $f = 5$ kHz; dotted line is a non-linear simulation using our model.

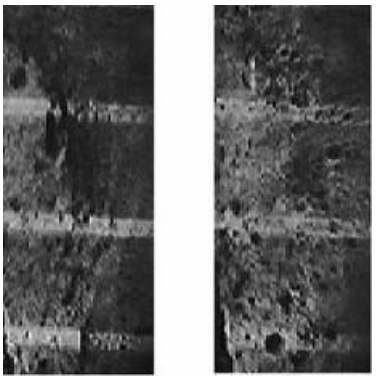

Figure 9. Microscopic images of the cell (PS treatment): before (on the left) and after (on the right) overheating to 85°C during 30 min (LC nematic–isotropic transition temperature T_{NI}=70°C).

corresponding unit vectors $\mathbf{n}_i$ and angles φ_i between $\mathbf{n}_0$ (unit vector of initial orientation) and $\mathbf{n}_i$ (see figure 10). The first (bulk) layer is situated in the middle of the cell and is described by the usual hydrodynamics of a NLC taking into account the average direction of the long LC molecular axis—director $\mathbf{n}_b$. The second (surface) layer plays the intermediate role of connecting orientation structures imposed by the surface and by the bulk region of the cell. This layer has a quasi-homogeneous orientation with a surface director $\mathbf{n}_s$, that determines the boundary conditions for the bulk layer. The third very thin absorbed layer with a thickness in the range 1–10 molecular lengths defines the average direction (easy axis $\mathbf{n}_e$) of the long axes of molecules induced by an anisotropy of the molecular interactions at the boundary liquid crystal – solid (polymer). In the absence of external torques (e.g. from an electric field) the directions of the surface director and of the easy axis are the same, although they can differ when a strong field is applied to the LC layer.

The theoretical backgrounds of such an approach may include certain types of molecular models to be developed, since physical properties of a LC and some types of polar liquids in the surface layers are very different from those in the bulk phase [9–12]. Indeed, direct NMR studies show the visible slowing of translation and orientation diffusion in the surface-absorbed layers, both for the isotropic phase of the LC and for isotropic polar liquids [9, 11]. This confirms earlier results on the shear viscosity of polar liquids [10]. To some extent such effects can be related to the translational and orientational ordering induced by the surface. The principal questions for a nematic phase are: what are the nature and the spatial structures of the intermediate surface layer formally described by the $\mathbf{n}_s$ director? In the case of a contact LC–polymeric substrate, it is reasonable to connect its existence with translation diffusion in the vicinity of the surface. This means that the boundary between the surface and the bulk layer is not strictly localized, and so the material parameters of this layer can depend continuously on the distance from the boundary. Such an opportunity has been discussed previously regarding the surface dynamic problem at the weakly anchoring boundary LC–photopolymer [12]. The thickness h of this layer (estimated from experiments on the surface dynamics) is about 100 nm and decreases with increasing temperature to the LC–isotropic transition. This value is much higher than for LC boundary layers in the isotropic phase mentioned already (about several nanometres). So we have to consider a sub-layer model as a first approximation, as we have no adequate physical explanation of the LC orientation dynamics in all the sub-layers, and even the very division into these sub-layers is just a rough approximation of the real situation. Another mechanism (for example long range interaction between ordered systems of LC and dye

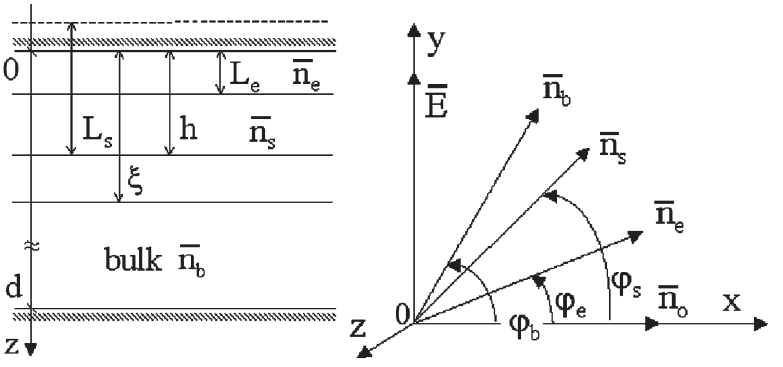

Figure 10. Sub-layered model of LC layers. $\mathbf{n}_0$=unit vector of initial orientation, $\mathbf{n}_e$=easy axis, $\mathbf{n}_s$=surface director, $\mathbf{n}_b$=bulk director, d=cell thickness, h=surface layer thickness, $\xi \sim d/E$=electric coherence length, $L_s=K_{22}/W_s$=the anchoring extrapolation length, $L_e=K_{22}/W_e$=extrapolation length of the easy axis.

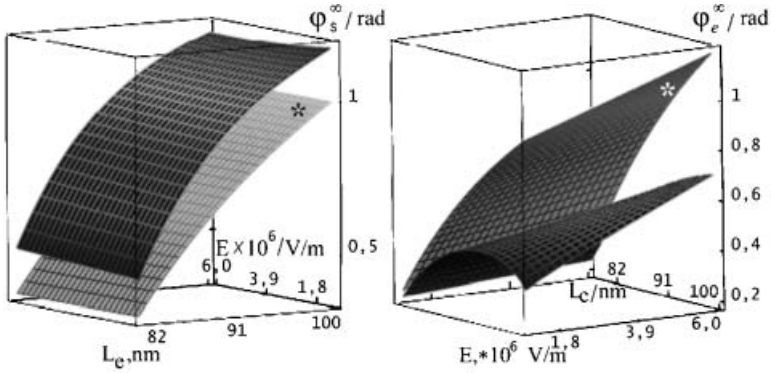

Figure 11. Dependence of the stationary angles φ_s^{∞} and φ_e^{∞} on the electric field strength and extrapolation length L_e^*,=linear solution, other=non-linear solution; parameters of calculation h=50 nm, L_s=100 nm, K_{22}=7.2E-12, $\Delta\varepsilon$=+3.4.

molecules on UV-treated photosensitive substrates) is now under consideration.

According to the geometry of our experiments the initial (planar) state of the LC layer corresponds to a homogeneous orientation ($\mathbf{n}_b=\mathbf{n}_s=\mathbf{n}_e$) along the x-axis parallel to the LC layer. After application of an electric field both the $\mathbf{n}_b$ and $\mathbf{n}_s$ directors rotate quickly to a new position defined by the field. Some phase delay between surface $\mathbf{n}_s$ and bulk $\mathbf{n}_b$ director rotations described by a surface viscosity $\eta_s=\gamma_1 h$ (γ_1 is the coefficient of a rotational viscosity, h is the thickness of the intermediate surface layer) can be detected at very high frequency of rotation (10^3–10^5 Hz) [11]. For the very slow phenomena under consideration this delay is negligible. Thus we may consider a synchronous rotation of $\mathbf{n}_s$ and $\mathbf{n}_b$ under the action of a strong electric field. In this case the bulk orientation is homogeneous ($\mathbf{n}_b \| \boldsymbol{E}$) everywhere except for the near surface layer with a thickness equal to the electric coherence length (figure 7):

$$\xi = (1/E)(K_{22}/\varepsilon_0\Delta\varepsilon)^{1/2} \tag{1}$$

where K_{22} is Frank's elastic module and $\Delta\varepsilon$ is the LC dielectric anisotropy. In this layer the orientation of $\mathbf{n}_b$ varies with the z-coordinate, approaching $\mathbf{n}_s$ in the intermediate surface layer (of thickness ξ) which can be considered as quasi-homogeneous. Thus an intensive electric field induces a rather strong twist deformation in the region between the bulk and intermediate surface layer, which can be referred as a torque Γ_b transmitted to the surface layer from the bulk. We obtain Γ_b from the expression for the free energy F of a LC layer contacted with a intermediate layer at $z=h$ [1]:

$$\Gamma_b = [\delta f/\delta(\partial\varphi/\partial z)]_s \tag{2}$$

where

$$\begin{aligned} F &= (1/2)\int_0^d f(\varphi, \partial\varphi/\partial z)\mathrm{d}z \\ &= (1/2)\int_0^d \left[K_{22}(\partial\varphi/\partial z)^2 - \varepsilon_0\Delta\varepsilon E^2\sin^2\varphi \right. \\ &\qquad \left. + W_s\cos^2(\varphi-\varphi_e)\delta(z)\right]\mathrm{d}z. \end{aligned} \tag{3}$$

The explicit form of the dependence $F(\varphi_s)$ can be approximately obtained using the reasonable function $\varphi(z)$ introduced in the model. Previously this dependence was approximated by linear [1] or by trigonometric functions [4]. We will use the previously proposed [1] linear approximation of the type:

$$\varphi(z) = A + Bz \tag{4}$$

with

$$A = [\varphi_s\xi - (\pi/2)h]/(\xi - h),\ B = [(\pi/2) - \varphi_s]]/(\xi - h) \tag{5}$$

which corresponds to the strong changes of orientation in the layer $h<z<\xi$ from a bulk value ($\varphi_b=\pi/2$ for $z>\xi$) to the surface value φ_s. We obtain a stationary value φ_s^{∞} for φ_s by putting the condition proposed in [8] for the

Table 1. 'Slow' times τ_1 and τ_2 derived from the approximation of $I(t)$ dependences by the two-exponential law: $I(t)=A_0+A_1\exp(-t/\tau_1)+A_2\exp(-t/\tau_2)$.

Surface treatment	Voltage/ V	Gap/ μm	t_{ex}/min/ min	τ_1/ min	τ_2/ min
PA	30	10	60	1.35	42
PA	50	100	720	5	145
PA	300	100	1050	29	636
PS	300	100	25	0.31	2.29
PS	300	100	50	0.57	7.43
PS	300	100	135	0.77	14.4

extrapolated linear function (4), which will be valid at least in the stationary case:

$$\varphi_s[z=-(L_s-h)]=0. \tag{6}$$

This results in:

$$\varphi_s^{\infty}=(\pi/2)L_s/[(L_s-h)+\xi] \tag{7}$$

where $L_s=K_{22}/W_s$, the anchoring extrapolation length corresponding to the anchoring strength W_s; it varies from few hundreds of Å for strong anchoring to some micrometers for very weak anchoring. We consider that in the general non-stationary case the expressions (6) and (7) can be changed. It easy to show using equations (3), (4) and (5) that for the case

$$\xi >> h, L \tag{8}$$

the density of the energy in the intermediate layer is mostly determined by the first elastic term in expression (3), and the second term corresponding to the electric field energy can be omitted. In this case we will obtain using equations (2–5):

$$\Gamma_b=K_{22}[(\pi/2)-\varphi_s]/(\xi-h). \tag{9}$$

The result obtained is similar to that reported previously [1], if inequality (8) is valid. The expression (9) can also be used, when ξ is comparable with h, if φ_s is small enough. Indeed it is easy to show that in this case the ratio R of electric elastic energy can be expressed as:

$$R=\{[\varphi_s(\xi-h)]/\xi[(\pi/2)-\varphi_s]\}^2. \tag{10}$$

For $\xi\cong 2h$, $\varphi_s\cong\pi/4$ we obtain $R\cong 0.25$ which seems to be small enough.

The torque Γ_b will be transmitted without change to the absorbed surface LC layer via an intermediate layer with a 'frozen' LC orientation, because the characteristic rotation time of the surface director $\mathbf{n}_s$ is fast in comparison with the slow relaxation process at the surface. So this mechanism initiates the slow rotation (gliding) of the easy axis.

The second opposite anchoring torque Γ_s applied to $\mathbf{n}_s$ from the absorbed layer can be easily expressed using equation (3) and taking into account that $\varphi=\varphi_s$ in the intermediate layer:

$$\Gamma_s=-(K_{22}/2L_s)\sin 2(\varphi_s-\varphi_e). \tag{11}$$

The viscous losses in the surface layer are described in terms of a surface viscosity Γ_s via surface viscous torque:

$$\Gamma_{vs}=-\gamma_s(\partial\varphi_s/\partial t). \tag{12}$$

So finally the equation of the torque balance acting on the surface director $\mathbf{n}_s$ can be expressed as

$$\begin{aligned}\Gamma_b+\Gamma_s+\Gamma_{vs}=&K_{22}[(\pi/2)-\varphi_s]/(\xi-h)\\&-(K_{22}/2L_s)\sin 2(\varphi_s-\varphi_e)\\&-\gamma_s(\partial\varphi_s/\partial t)=0.\end{aligned} \tag{13}$$

We can consider the balance of moments acting on the easy axis on the boundary between intermediate layer and absorbed layer in the same manner. In this case we must introduce the anchoring strength W_e and the reciprocal length $L_e=K_{22}/W_e$ of the easy axis in a similar manner, to write down the elastic moment Γ_e which prevents the gliding process:

$$\Gamma_e=-(K_{22}/2L_e)\sin 2\varphi_e. \tag{14}$$

The driven torque Γ_b transmitted from the bulk is defined by expression (9). We also can formally introduce the viscous torque Γ_{ev} for the easy axis gliding as:

$$\Gamma_{ve}=-\gamma_e(\partial\varphi_e/\partial t). \tag{15}$$

we consider the viscosity of gliding γ_e as a parameter which reflects the complicated processes of absorption and desorption in the absorbed layer [4]. In this case we can write the balance equation for torques acting on the easy axis (we suggest $L_e\sim h$):

$$\begin{aligned}&K_{22}[(\pi/2)-\varphi_s]/(\xi-h)-(K_{22}/2L_e)\sin 2\varphi_e\\&-\gamma_e(\partial\varphi_e/\partial t)=0.\end{aligned} \tag{16}$$

The presented system of coupled equations (13) and (16), represents the complex character of the influence of an electric field on the easy axis, which is transmitted via the intermediate surface layer (of thickness h). In this case the interaction between different sub-layers plays an important role. It may be noted that the non-linear character of the equations presented must be taken into account, both for stationary and dynamic regimes of field-induced orientational changes. This is illustrated by figure 11, as the result of a comparison between linear and non-linear stationary solutions $\varphi_s^{\infty}=\varphi_s(t\to\infty)$ and $\varphi_e^{\infty}=\varphi_e(t\to\infty)$ of the system (13), (16). In this case the system given above can be transformed to the dimensionless form convenient for

numerical calculations:

$$L_s^*\left[(\pi/2)-\varphi_s^\infty\right]-(1/2)\sin 2\left(\varphi_s^\infty-\varphi_e^\infty\right)=0 \quad (17)$$

$$L_e^*\left[(\pi/2)-\varphi_s^\infty\right]-(1/2)\sin 2\varphi_e^\infty=0 \quad (18)$$

where

$$L_{s(e)}^*(\xi)=L_{s(e)}/(\xi-h). \quad (19)$$

It is easy to show that a linear solution for φ_e^∞ can be written by an expression similar to (7):

$$\varphi_e^\infty=(\pi/2)\{L_e/[(L_s-h)+\xi]\}. \quad (20)$$

So the angles φ_s^∞ and φ_e^∞ vary with electric field in a similar manner, via dependence $\xi(\mathbf{E})$. Our estimates have shown that the non-linearity may play an essential role at $\varphi_s^\infty\left(\varphi_e^\infty\right)\geq 10^0$.

Linear solutions of the system (13), (16) describe certain details of a LC gliding dynamics at the turning on and off of an electric field. It is shown in the Appendix that in both cases the characteristic time of gliding τ_e can be expressed as:

$$\tau_e=\tau_e^0\left[\left(L_s^*+C_1\right)\right]/\left[C_2\left(L_s^*+C_1\right)+L_e^*C_1\right] \quad (21)$$

where $C_1=\cos 2\left(\varphi_s^\infty-\varphi_e^\infty\right)$, $C_2=\cos 2\varphi_e^\infty$, and the considerable difference between 'slow' τ_e^0 and 'fast' τ_s^0 times has been taken into account:

$$\tau_e^0=(\gamma_e L_e)/K_{22} >> \tau_s^0=(\gamma_s L_s)/K_{22}. \quad (22)$$

Indeed, it is easy to show that for reasonable values of parameters entered into the model ($W_s\sim 10^{-5}\,\mathrm{J\,m^{-2}}$, $L_s\sim h\sim 10^{-7}\,\mathrm{m}$, $K_{22}\sim 10^{-11}\,\mathrm{N}$, $\gamma_s=\gamma_1 h\sim 10^{-8}\,\mathrm{Pa\,s\,m}$) the characteristic time τ_s^0 is about 1 ms and such fast variations cannot be responsible for the slow process attributed to the easy axis gliding with characteristic time τ_e^0.

Let us consider small disturbances, i.e. $|\varphi_s^\infty|$, $|\varphi_e^\infty|\ll 1$, $C_1\cong C_2\cong 1$ in equation (21). On turning on the electric field the characteristic time of gliding τ_e^{on} decreases with increasing $\mathbf{E}$ mostly due to the dependence $L_{s(e)}^*(\xi)$ but the rate of such decrease depends on the relationship between characteristic lengths entering into the model (figure 10). For larger stationary values of φ_s^∞ and φ_e^∞ a more complicated dependence $\tau_e^{on}(E)$ is possible due to the dependence $C_{1(2)}(\xi)$. In the case of turning off the electric field one has to put $\xi\approx d\gg h$, $L_{s(e)}$ and the relaxation time of gliding,

$$\tau_e^{off}\cong\tau_e^0/C_2\cong\tau_e^0 \quad (23)$$

will exceed the 'turn on' time τ_e^{on}, which is in an accordance with our experimental data.

Although the LC layer thickness enters into the general expression (21) variation in this parameter do not lead to the variation of the relaxation time τ_e^{off}, as d is considerably greater than the thickness of boundary layers. This explains the independence of the slow surface dynamics of the local thickness of the experimental layer.

The independence of τ_e^{off}, equation (23), of the voltage and of the excitation time contradicts the results of our experiments. Indeed, an analysis of the experimental results shows that the slow relaxation times τ_1 and τ_2 derived from experimental curves $I(t)$ (see table 1) increase with increasing t_{ex} roughly in accordance with a simple law: $\tau_{1(2)}\sim t_{ex}$ for both types of weakly anchoring surfaces. The application of more general non-linear equations (13), (16) does not help to explain this contradiction. The example of non-linear numerical calculations of $I(t)$ is presented in figure 8. To obtain the theoretical curve the time dependence of the angle was transformed into time dependence $I(t)$ of the intensity of light passing through crossed polarizers. We took into account that after turning off the electric field the wave-guided regime [6] is valid for the experimental parameters. So we can write for the output intensity $I(t)$ the simple expression:

$$I(t)=I_0\sin^2\varphi_e(t). \quad (24)$$

The result of the comparison of experimental and theoretical non-linear dependences $I(t)$ shown in figure 8 reveals that the existence of two exponential laws can be referred to the non-linear character of the dynamical equations. This law cannot be described in the linear approximation, as for turning off the electric field it predicts:

$$I(t)\sim\varphi_e^2(t)\sim\exp\left(-2t/\tau_e^{off}\right). \quad (25)$$

In the calculations we used the material parameters of ZhK 616 ($\Delta\varepsilon=+3.4$, $K_{22}=7.2\times 10^{-12}\,\mathrm{N}$) and set the final level of the light intensity connected with memory effects as a constant contribution, which does not enter into the model. The values obtained for the surface viscosity (6 Pa s m) at lengths $L_s=100\,\mathrm{nm}$, $L_e=90\,\mathrm{nm}$, $h=50\,\mathrm{nm}$ seem to be reasonable, taking into account the previously obtained results [1, 4]. Similar calculations for the case of polystyrene films show that obtained values of γ_e are sometimes lower for the same approximation lengths.

Despite the fact that the non-linearity really provides a better qualitative explanation of the experimental results (dotted curve in figure 8), the proposed model is too approximate to describe the dependence of τ_e^{off}, in equation (25), on the exposure time t_{ex} and electric field amplitude (see table 1). The effects of the permanent memory registered in our experiments are also out of

prediction of such a simple model and demand a deeper insight into the problem. This can be done on the basis of microscopic approaches. In particular, it is possible to modify the orientational diffusion model [13] applied previously to explain complicated slow dynamics and memory effects in the surface layer of an azo-dye. Account can thus be taken of the structural transformations of the aligning surface due to its interaction with the anisotropic LC potential [5]. Additional experiments with different types of weakly anchoring surfaces are also of importance.

5. Conclusion

New results of experimental investigations of azimuthal director reorientation dynamics for a nematic liquid crystal on solid substrates are shown for two types of substrate with weak anchoring: glass/polystyrene and glass/UV-activated dye. Slow and fast relaxation processes were observed in both cases. The slow surface reorientation and memory effects were controlled by two parameters: the electric voltage and the excitation time. A dependence on the anchoring strength for UV-treated surfaces was also observed.

The proposed sub-layered phenomenological model provides a qualitative explanation of some experimental results. Nevertheless the physical origin of gliding phenomena can be clarified only by using microscopic models, which are now under consideration. Our experiments have shown that the values of the conventional viscosity of gliding, which reflect the speed of absorption, are different for different types of surface treatment.

Acknowledgements

This research was partially supported by RGC grants HKUST6102/03E, HKUST6149/04E, and DAG grant DAG05/06.EG14. We wish to thank H.S. Kwok and V.M. Kozenkov for fruitful discussion.

References

[1] V.P. Vorflusev, H.S. Kitzerow, V.G. Chigrinov. *Appl. Phys. Lett.*, **70**, 3359 (1997).
[2] E.A. Oliveira, A.M. Figueiredo, G. Durand. *Phys.Rev. A*, **44**, R825 (1991).
[3] S. Faetti, M. Nobili, I. Raggi. *Eur. Phys. J. B*, **11**, 445 (1999).
[4] S. Joly, K. Antonova, P. Martinot-Lagarde, I. Dozov. *Phys. Rev. E*, **70**, 050701 (2004).
[5] I. Janossy, T.J. Kosa. *Phys. Rev. E*, **70**, 052701 (2004).
[6] V.G. Chigrinov. *Liquid Crystal Devices: Physics and Applications*. Artech House, Boston (1999).
[7] S.V. Pasechnik, V.G. Chigrinov, D.V. Shmeliova, V.A. Tsvetkov, A.N. Voronov. *Liq. Cryst.*, **31**, 585 (2004).
[8] G.E. Durand, E.G. Virga. *Phys. Rev. E*, **59**, 4137 (1999).
[9] G.P. Crawford, D.K. Yang, S. Zumer, D. Finotello, J.W. Doane. *Phys. Rev. Lett.*, **66**, 723 (1991).
[10] B.Y. Derjaguin, YU. M. Popovskij, B.A. Altoiz. *J. Colloid Interface Sci.*, **96**, 492 (1983).
[11] J.-P. Korb, L. Malier, F. Cros, S. Xu, D.J. Jonas. *Phys. Rev. Lett.*, **77**, 2312 (1996).
[12] M. Vilfan, I. Drevensek, A. Mertelj, M. Copic. *Phys. Rev. E*, **63**, 061709 (2001).
[13] V. Chigrinov, S. Pikin, A. Verevochnikov, V. Kozenkov, M. Khazimullin, J. Ho, D.D. Huang, H.S. Kwok. *Phys. Rev. E*, **69**, 061713–1 (2004).

Appendix

Linearization of non-linear dynamic equations (13), (16) with stationary values φ_s^{∞}, φ_e^{∞} can be made as follows:

$$\varphi_s(t) = \varphi_s^{\infty} + \varphi_s^*(t) \tag{A1}$$

$$\varphi_e(t) = \varphi_e^{\infty} + \varphi_e^*(t) \tag{A2}$$

where $\varphi_s^*(t)$, $\varphi_e^*(t)$ are small angles.

Let us consider that after some disturbance of the system by step-like changes of ξ (from ξ^- to ξ^+) at $t=0$ (induced by an abrupt change of electric field **E**) this system will relax to the new stationary state so that:

$$\varphi_s^*, \varphi_e^* \to 0, \text{ at } t \to \infty. \tag{A3}$$

This means that the asymptotic values of the angles $\varphi_s(t)$, $\varphi_e(t)$ at $(t \to \infty)$ are the same as stationary values φ_s^{∞} and φ_e^{∞} obtained from the system (17), (18) for the values of $L_s^*(\xi^+)$, $L_e^*(\xi^+)$ correspondent to the stage $t>0$ (after changing of **E** and ξ).

The initial conditions for $\varphi_s(t)$ and $\varphi_e(t)$ are

$$\varphi_s^*(0) = \varphi_s^- - \varphi_s^{\infty} \tag{A4}$$

$$\varphi_e^*(0) = \varphi_e^- - \varphi_e^{\infty} \tag{A5}$$

where φ_s^-, φ_e^- are the stationary solutions of the system (17), (18) for values of $L_s(\xi^-)$, $L_e(\xi^-)$ corresponding to the stage $t \le 0$ (before changing **E** and ξ).

For linearized equations derived from (13), (16) we may write:

$$\begin{aligned}&[K_{22}/(\xi - h)]\varphi_s^* + \left[(K_{22}/L_s)\cos 2\left(\varphi_s^{\infty} - \varphi_e^{\infty}\right)\right] \\ &\left(\varphi_s^* - \varphi_e^*\right)\left] + \gamma_s\left(\partial\varphi_s^*/\partial t\right) = 0\right.\end{aligned} \tag{A6}$$

$$\begin{aligned}&[K_{22}/(\xi - h)]\varphi_s^* + \left[(K_{22}/L_e)\cos 2\varphi_e^{\infty}\right]\varphi_e^* \\ &+ \gamma_e\left(\partial\varphi_e^*/\partial t\right) = 0.\end{aligned} \tag{A7}$$

To define a fast motion of the surface director ($\mathbf{n}_s$) and a slow rotation of an easy axis ($\mathbf{n}_e$), we introduce

fast (τ_s^0) and slow (τ_e^0) characteristic times determined by the equation (22) and transform equations (A6), (A7) into a more compact form by using parameters introduced above. In this case we obtain the following linear system:

$$\left(L_s^* + C_1\right)\varphi_s^* - C_1\varphi_e^* + \tau_s^0\left(\partial\varphi_s^*/\partial t\right) = 0 \tag{A8}$$

$$L_e^*\varphi_s^* + C_2\varphi_e^* + \tau_e^0\left(\partial\varphi_e^*/\partial t\right) = 0 \tag{A9}$$

where:

$$C_1 = \cos 2\left(\varphi_s^\infty - \varphi_e^\infty\right) \tag{A10}$$

$$C_2 = \cos 2\varphi_e^\infty. \tag{A11}$$

This system can be easily solved by a Laplace transform. The algebraic equations for Laplace-images $\Phi_s = L\{\varphi_s^*\}$ and $\Phi_e = L\{\varphi_e^*\}$ of the functions φ_s^* and φ_e^* are presented as:

$$\left(L_s^* + C_1 + \tau_s^0 s\right)\Phi_s - C_1\,\Phi_e = \tau_s^0\varphi_s^*(0) \tag{A12}$$

$$L_e^*{}_s + \left(C_2 + \tau_e^0 s\right)_e = \tau_e^0\varphi_e^*(0). \tag{A13}$$

The characteristic determinant D of this system can be expressed in the form:

$$D = \tau_s^0\tau_e^0(s - s_1)(s - s_2) \tag{A14}$$

where:

$$\begin{aligned} s_{1,2} = \Big\{ &- \left[\left(L_s^* + C_1\right)\tau_e^0 + C_2\tau_s^0\right] \pm \\ &\left[\left(L_s^* + C_1\right)\tau_e^0 - C_2\tau_s^0\right][1-\beta]^{1/2}\Big\} \Big/ \left(2\tau_s^0\tau_e^0\right) \\ = \Big\{ &- \left[\left(L_s^* + C_1\right) + C_2\alpha\right] \pm \\ &\left[\left(L_s^* + C_1\right) - C_2\alpha\right][1-\beta]^{1/2}\Big\} \Big/ \left(2\alpha\tau_e^0\right) \end{aligned} \tag{A15}$$

with the dimensionless parameters:

$$\begin{aligned} \alpha &= \tau_s^0/\tau_e^0 = (\gamma_s L_s)/(\gamma_e L_e) \\ \beta &= \left(4\tau_s^0\tau_e^0 L_e^* C_1\right)\Big/\left[\left(L_s^* + C_1\right)\tau_e^0 - C_2\tau_s^0\right]^2 \\ &= \left(4\alpha L_e^* C_1\right)\Big/\left[\left(L_s^* + C_1\right) - C_2\alpha\right]^2. \end{aligned} \tag{A16}$$

It is easy to show that in the case of a considerable difference between 'fast' and 'slow' times:

$$\alpha = \tau_s^0/\tau_e^0 << 1 \tag{A17}$$

$$\beta << 1. \tag{A18}$$

The roots s_1, s_2 correspond to the slow and fast relaxation modes with characteristic times

$$\begin{aligned} \tau_e &= -(1/s_1) \cong \\ &\tau_e^0\left[\left(L_s^* + C_1\right)\right]\Big/\left[\left(C_2\left(L_s^* + C_1\right) + L_e^* C_1\right)\right] \end{aligned} \tag{A19}$$

$$\tau_s = -(1/s_2) \cong \tau_s^0\Big/\left(L_s^* + C_1\right). \tag{A20}$$

The solution of the system (A12), (A13) can be expressed in the usual manner as:

$$\Phi_{s(e)} = D_{s(e)}/D \tag{A21}$$

where

$$D_s = \left(C_2\tau_e^0 s\right)\tau_s^0\varphi_s^*(0) + C_1\tau_e^0\varphi_e^*(0) \tag{A22}$$

$$D_e = \left(L_s^* + C_1 + \tau_s^0 s\right)\tau_e^0\varphi_e^*(0) - L_s^*\tau_s^0\varphi_s^*(0). \tag{A23}$$

The obtained solutions, (A22) (A23), can easily be transformed to a form convenient for a reverse Laplace transform:

$$\Phi_{s(e)} = \left[A_{s(e)} + B_{s(e)}s\right]\Big/\left[\tau_s^0\tau_e^0(s - s_1)(s - s_2)\right] \tag{A24}$$

where

$$A_s = C_2\tau_s^0\varphi_s^*(0) + C_1\tau_e^0\varphi_e^*(0) \tag{A25}$$

$$B_s = \tau_e^0\tau_s^0\varphi_s^*(0) \tag{A26}$$

$$A_e = \left(L_s^* + C_1\right)\tau_e^0\varphi_e^*(0) - L_s^*\tau_s^0\varphi_s^*(0) \tag{A27}$$

$$B_e = \tau_s^0\tau_e^0\varphi_e^*(0) - L_s^*\tau_s^0\varphi_s^*(0). \tag{A28}$$

Using the reverse Laplace transform, the functions $\varphi_s^*(t)$ and $\varphi_e^*(t)$ can be expressed as:

$$\begin{aligned} \varphi_{s(e)}^*(t) = \Big\{ &\left[A_{s(e)} + B_{s(e)}s_1\right]\exp(s_1 t) - \\ &\left[A_{s(e)} + B_{s(e)}s_2\right]\exp(s_2 t)\Big\}\Big/\left[\tau_s^0\tau_e^0(s_1 - s_2)\right] \end{aligned} \tag{A29}$$

where s_1 and s_2 are determined in the general case by equation (A15).

In the particular case of a considerable difference between slow and fast times, (A17) (A18):

$$s_1 - s_2 \cong -s_2 = \left(C_1 + L_s^*\right)/\tau_s^0 \tag{A30}$$

$$A_s \cong C_1\tau_e^0\varphi_e^*(0) \tag{A31}$$

$$A_e \cong \left(L_s^* + C_1\right)\tau_e^0\varphi_e^*(0). \tag{A32}$$

And we obtain the following approximate solutions neglecting the terms with $\alpha \ll 1$ (A17):

$$\varphi_s^*(t) \cong \left\{ C_1 \varphi_e^*(0) \exp(-t/\tau_e) - \left[C_1 \varphi_e^*(0) - \left(C_1 + L_s^* \right) \varphi_s^*(0) \right] \exp(-t/\tau_s) \right\} / \left(C_1 + L_s^* \right) \quad \text{(A33)}$$

$$\varphi_e^*(t) \cong \varphi_e^*(0) \exp(-t/\tau_e) \quad \text{(A34)}$$

where the relaxation times τ_s and τ_e are determined by equations (A19), (A20).

Thus, for the surface director $\mathbf{n}_s$ the relaxation includes two stages (fast and slow) with considerably different characteristic times. At the same time, the slow relaxation alone dominates in the solution for the easy axis. Intuitively one has to wait this type of behaviour for the proposed layered model. In the particular case of linear distortions of the director induced by turning on or off an electric field relative to the states with small angles φ_s^∞ and φ_e^∞, we have: $C_1 \cong C_2 \cong 1$. Thus the expressions for the times of slow relaxation of the easy axis in the case of turning on and off the electric field can be written as:

$$\tau_{on} = \tau_e(\xi) = (\gamma_1 L_e) / \{ K_{22} [1 + L_e / (L_s - h + \xi)] \} \quad \text{(A35)}$$

and

$$\tau_{off} = \tau_e(\xi = d) = (\gamma_1 L_e) / \{ K_{22} [1 + L_e / (L_s - h + d)] \}. \quad \text{(A36)}$$